Electronic Supplementary Material (ESI) for Inorganic Chemistry Frontiers.

Supplementary material to:

Hybrid molecular-inorganic materials: Heterometallic [Ni_4Tb] complex grafted on superparamagnetic iron oxide nanoparticles

*Lidia Rosado Piquer,[a] Erika Jiménez Romero,[c] Yanhua Lan,[b] Wolfgang Wernsdorfer,[b] Guillem Aromí,[a] E. Carolina Sañudo[a,]**

[a] Departament de Química Inorgànica i Institut de Nanociència i Nanotecnologia, Universitat de Barcelona. Av. Diagonal 645, 08028 Barcelona, SPAIN. [b] CNRS and Université Grenoble Alpes, Institut Néel, 38042 Grenoble, FRANCE [c] European Synchrotron Radiation Facility, ID32, 71 Av. des Martyrs, Grenoble, France.

Materials and methods

[$Ni(OH)_2$]·xH_2O: A solution of $NiCl_2 \cdot 6H_2O$ (2.59 g, 10.88 mmol) and NaOH (0.870 g, 21.76 mmol) in 50 ml of water was stirred for 10 minutes. The green precipitate was filtered and dried for circa 12 - 20 hours in vacuum. Yield: quantitative. IR data (KBr, cm^{-1}): 3488 (s, b), 2356 (m), 2329 (w), 1645 (m), 1462 (m), 1369 (m), 655 (s, b), 416 (s); where strong (s), medium (m), weak (w), broad (b).

Elemental analyses (CHN) were performed at Servei de Microanàlisi in CSIC (Consell Superior d'Investigacions Científiques). Infrared spectra were collected on KBr pellets on an AVATAR 330 FT-IR at Departament de Química Inorgànica, Universitat de Barcelona.

X-Ray diffraction data were collected on a Bruker APEXII SMART diffractometer using Molybdenum Kα microfocus (λ=0.71073Å) radiation source. The structures were solved by Patterson methods (SHELXS2013) and refined on F^2 (SHELXL-

2013). Hydrogen atoms were included on calculated positions, riding on their carrier atoms. Cif files can be obtained free of charge from the Cambridge Structural Database (http://www.ccdc.cam.ac.uk/, deposition numbers 1455786 and 1455787).

Magnetic measurements were performed at the Unitat de Mesures Magnètiques of the Universitat de Barcelona on a Quantum Design SQUID MPMS-XL magnetometer equipped with a 5 T magnet. Diamagnetic corrections for the sample holder and for the sample using Pascal's constants were applied. Hysteresis measurements were performed with an array of micro-SQUIDs. This magnetometer works in the temperature range of 0.04 to 5 K and in fields up to 1.4 T with sweeping rates as high as 0.28 T s^{-1}. Dynamic Light Scattering (DLS): A Zetasizer NanoS Spectrometer was used for the Dynamic Light Scattering (DLS) measurements. The samples were measured in quartz cuvettes. Transmission Electron Microscopy: Specimens were analyzed using a JEOL JEM-2100 LaB6 transmission electron microscope with energy dispersed analysis of X-Rays (EDX), operating at 200 kV. The spectrometer is an Oxford Instruments INCA x-sight, with Si (Li) detector, acquisition was accomplished using the INCA Microanalysis Suite version 4.09 software. Images were recorded with Gatan CCD Camera Orius SC1000 and Digital Micrograph v.1.82.80 software.

X-Ray Magnetic Circular Dichroism spectra measured at the Ni $L_{2,3}$, Fe $L_{2,3}$ and Tb $M_{4,5}$-edges were obtained in the total electron yield (TEY) mode at the soft X-ray ID32 beamline at ESRF, Grenoble.[24] The measurements were performed in ultra-high vacuum chamber at 5 K in an applied magnetic field of 9 T along the x-ray beam propagation. The XMCD spectra were obtained by taking the difference of two XAS spectra with the x-ray helicity reversed while the magnetic field was held fixed. This corresponds to the difference between antiparallel and parallel alignments of the helicity and magnetization. XAS spectra have been normalized to the incident photon intensity. XMCD spectra were normalized to the XAS edge jump at the L and M edge.

Table S1. Crystallographic and data collection information for complexes **Ni₄Tb** and **Ni₄La**.

Identification code	Ni_4Tb	Ni_4La
Crystal system	monoclinic	monoclinic
Space group	$P2_1/c$	$P2_1/c$
a/Å	20.3895(7)	20.432(3)
b/Å	33.1075(12)	33.212(5)
c/Å	21.0870(8)	21.126(3)
α/°	90.00	90.00
β/°	115.982(2)	115.150(8)
γ/°	90.00	90.00
Volume/$Å^{3}$	12796.0(8)	12976.8
Z	4	4
Final R indexes [I≥2σ (I)]	R_1= 0.0772 wR_2= 0.2043	R_1= 0.0758 wR_2= 0.2131
T/K	100 K	100 K

Figure S1. Crystal structure of Ni_4La.

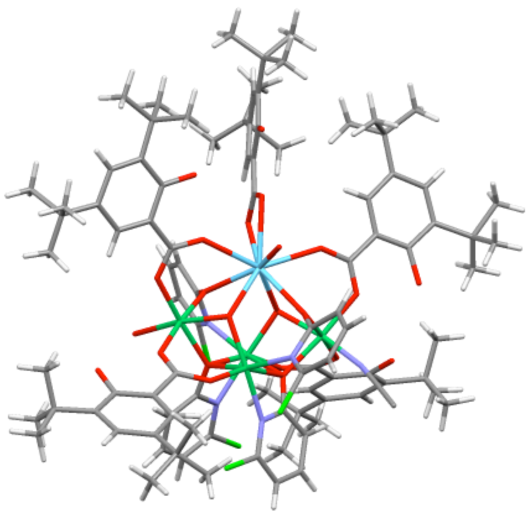

Figure S2. (a) Magnetization vs. field plots for Ni_4Tb at different temperatures (2 K, 4 K, 8 K, 10 K and 15 K). (b) AC magnetic susceptibility for Ni_4Tb at 100 Hz with applied dc fields of 1000-2500 Oe.

(a)

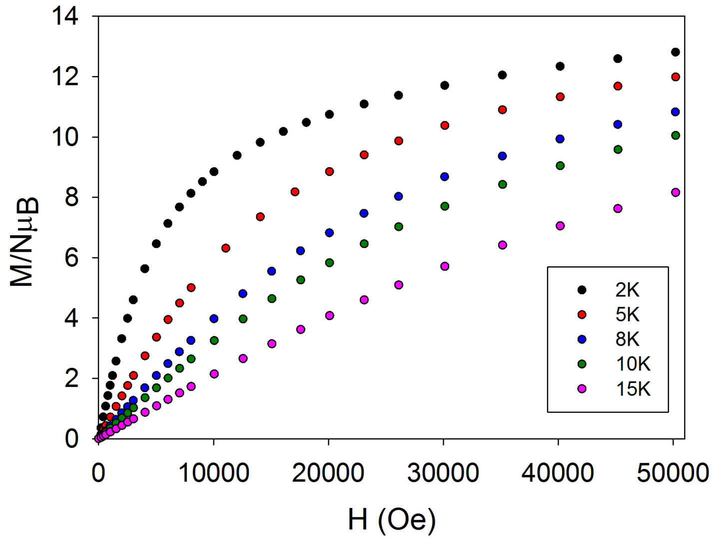

(b)

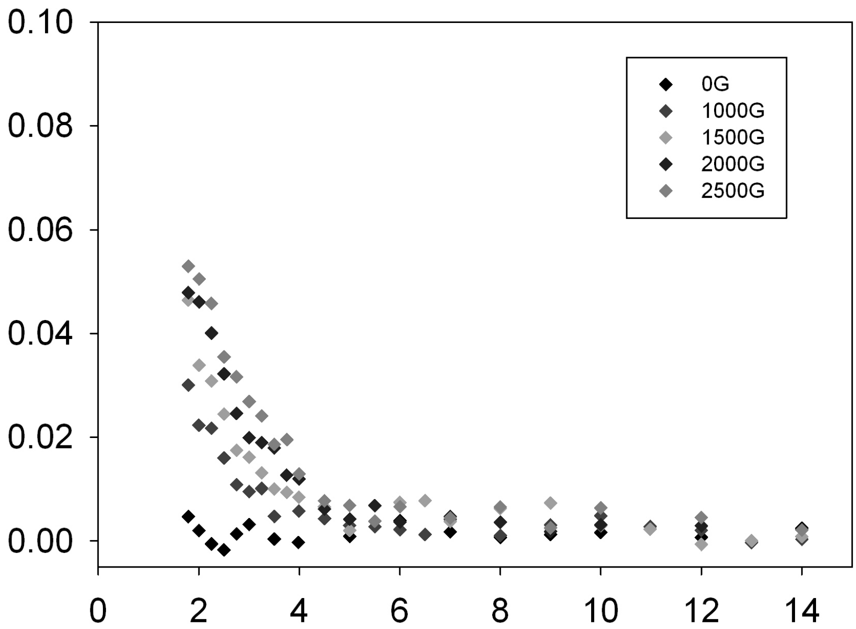

Figures S3. MicroSQUID magnetization vs. field hysteresis at various temperatures and field-scan rates for Ni_4Tb. The magnetization is normalized to its saturation value M_s.

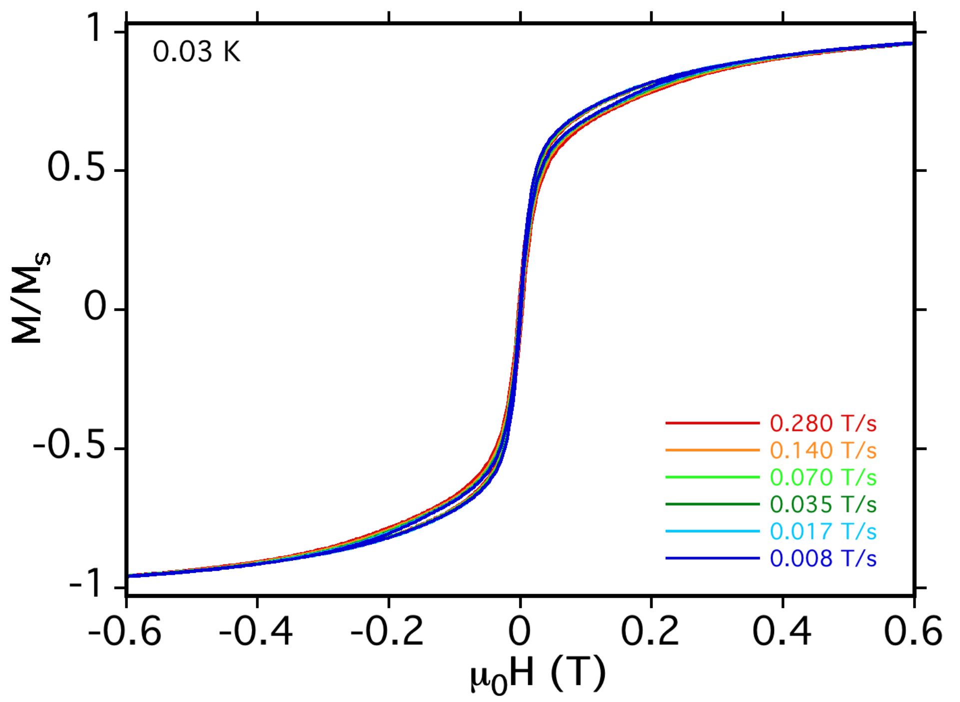

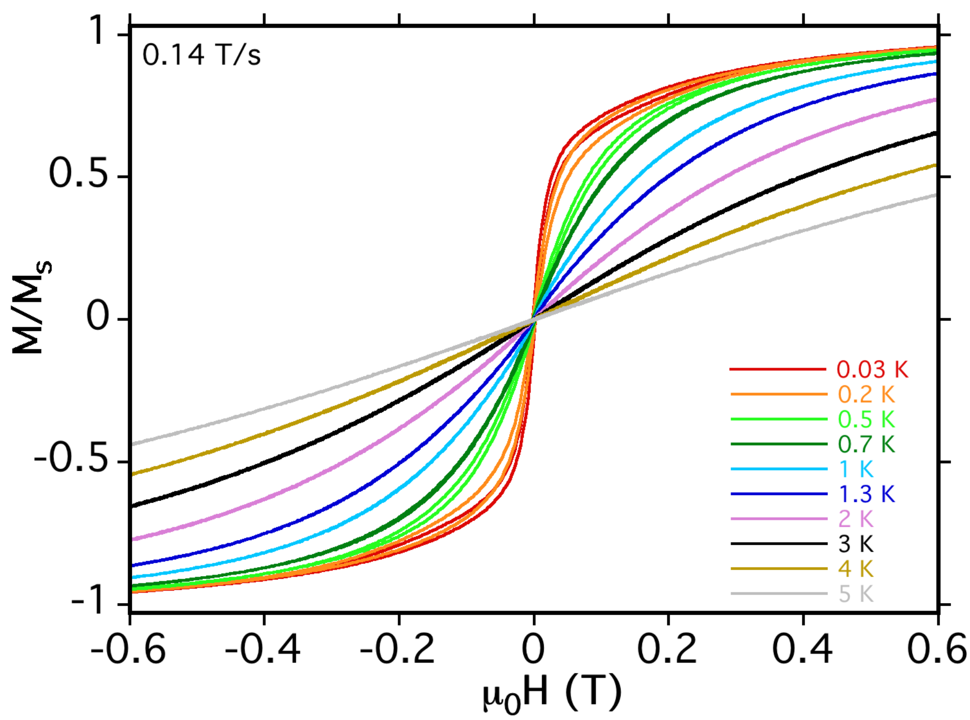

Figure S5. Zoom of the -1000 to 1000 Oe region of the field cooled (FC) magnetization vs. field at 2 K for the hybrid system NP-Ni_4Tb at FC = 0.2 T, 0.5 T and 5 T.

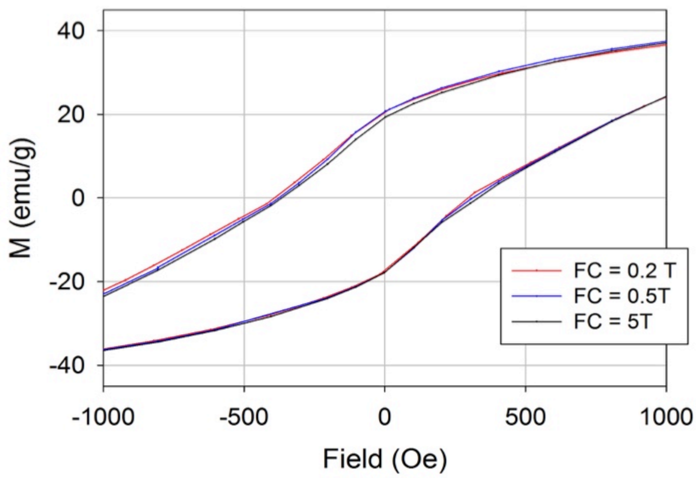

Figure S6. Variation of the XMCD spectra of pure Ni_4Tb at Ni and Tb-edges with the magnetic field from 9 T to -9 T in steps of one T. The data are also plotted as XMCD signal vs. field, or element specific hysteresis loops for Ni and Tb.

Ni-edge

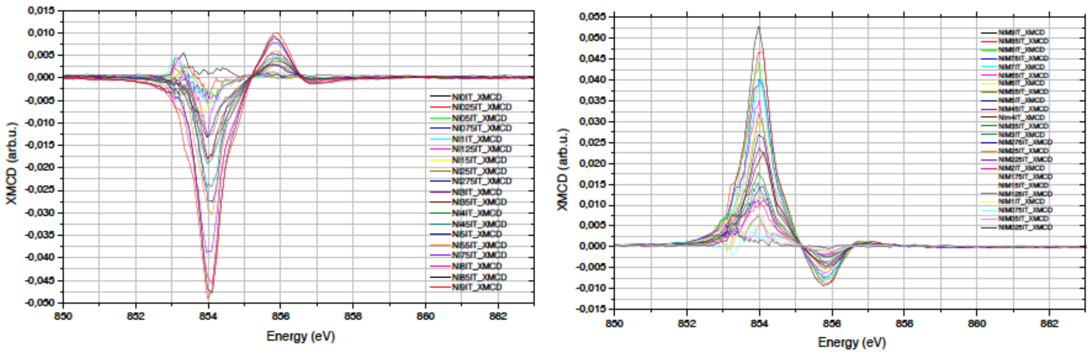

Tb-edge

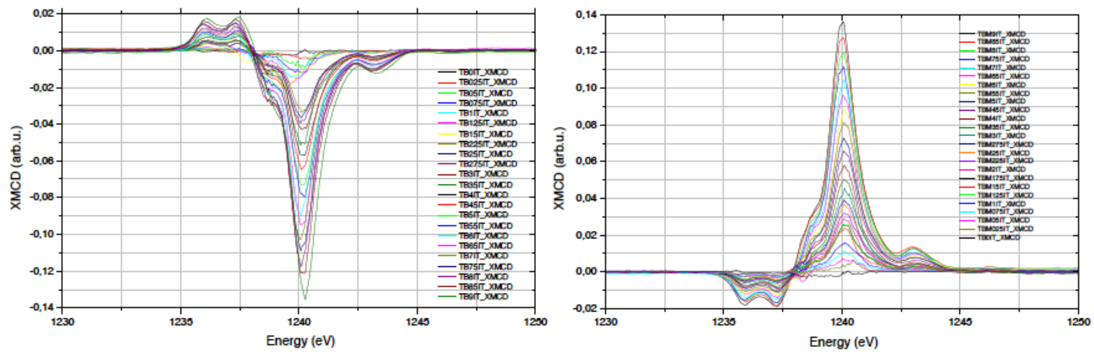

Ni edge

Tb edge

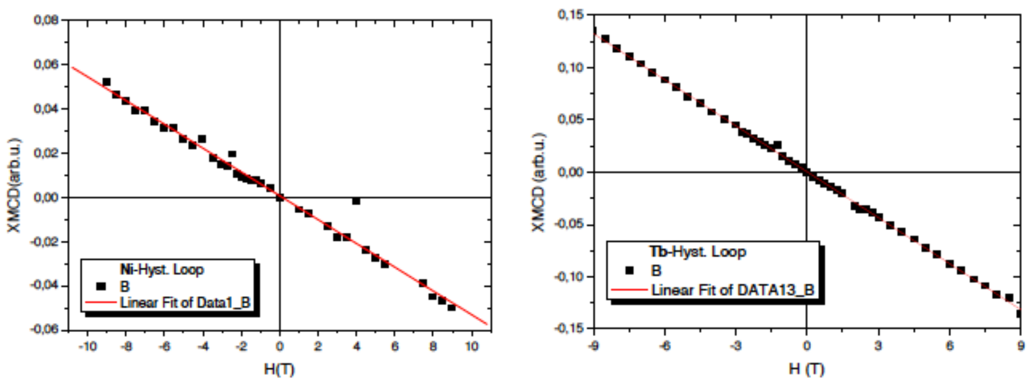

Figure S7. (a) XMCD at Fe-edge for the NP-Ni_4Tb hybrid system. A small amount of oxidation is observed after several months of storage in atmospheric conditions. (b) Variation of the XMCD signal at Fe edge for the NP-Ni_4Tb hybrid material between 5 T and -5 T at steps of 1 T.

(a)

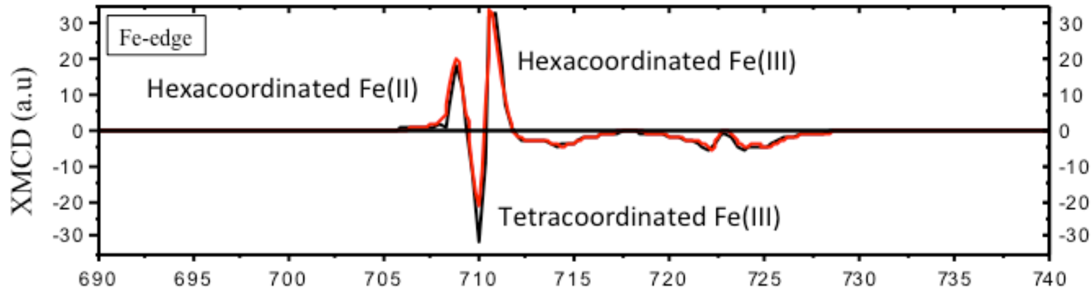

(b)

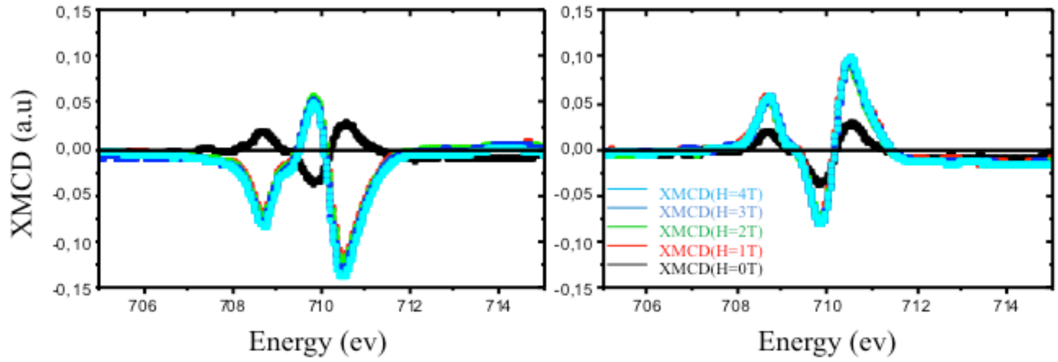

Figure S8. Variation of the XMCD signal at Tb edge for the NP-Ni_4Tb hybrid material between 4 T and -4 T. The small 1 eV shift is within the noise level of the averaging method.

Tb edge (negative field, top; positive field, bottom)